

# Enzyme-enhanced CO<sub>2</sub> capture in carbonate solution using hollow fiber membrane contactors: A novel numerical approach

Mohamed Nadir Khelifi<sup>1\*</sup>, Ouacil Saouli<sup>1</sup> and Zineb Boutamine<sup>1</sup>

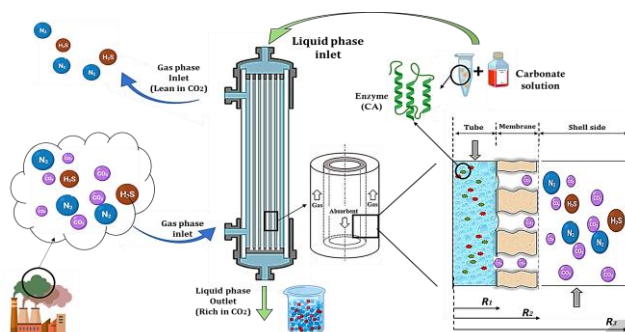
<sup>1</sup>Laboratoire de Génie des Procédés pour le Développement Durable et les Produits de Santé (LGPDDPS), Ecole Nationale Polytechnique de Constantine, Algeria.

Received: 18/03/2025, Accepted: 14/05/2025, Available online: 26/05/2025

\*to whom all correspondence should be addressed: nadir.khelifi@doctorant1.enp-constantine.dz

<https://doi.org/10.30955/gnj.07470>

## Graphical abstract



## Abstract

Due to the widespread use of fossil fuels, atmospheric levels of carbon dioxide (CO<sub>2</sub>), a major contributor to climate change, have increased dramatically. Through the simulation of a two-dimensional (2D), bovine carbonic anhydrase (bCA)-mediated mechanism, this work presents a novel approach method for CO<sub>2</sub> capture using membrane contactor, the technique uses aqueous carbonate solution as a chemical solvent. It is tested both with and without bCA. The influence of important parameters on the CO<sub>2</sub> capture performance, such as gas flow rate, liquid flow rate, bCA concentration in both counter- and co-current flow are investigated. The results show that the addition of 5 mg L<sup>-1</sup> bCA improves the removal efficiency by 24%, it is found that increasing the gas flow rate of CO<sub>2</sub> from 10 mL min<sup>-1</sup> to 40 mL min<sup>-1</sup> reduces the CO<sub>2</sub> removal from 23.47% to 6.68% in pure solution, whereas with 5 mg L<sup>-1</sup> bCA increasing the gas flow rate of CO<sub>2</sub> from 10 mL min<sup>-1</sup> to 40 mL min<sup>-1</sup> reduces the CO<sub>2</sub> removal from 57.17% to 19.79%. Increasing the liquid flow rate from 10 mL min<sup>-1</sup> to 40 mL min<sup>-1</sup> increases the CO<sub>2</sub> removal from 23.47% to 56.33% without the addition of bCA, with 5 mg L<sup>-1</sup> bCA the CO<sub>2</sub> removal increases from 57.17% to 69.07%. The counter-current is better than the co-current by 3% improvement. The effect of the bCA enzyme on CO<sub>2</sub> capture is limited by the availability of CO<sub>2</sub> (the substrate) and the catalytic capacity of the enzyme. The proposed simulation approach for maximum enzyme concentration, incorporates kinetic effects while maintaining the same parameters and

operating conditions as reported in the literature, maximum CO<sub>2</sub> removal efficiency, approaching almost total removal, is achieved at an enzyme concentration of approximately 30 mg L<sup>-1</sup> for the same CO<sub>2</sub> load.

**Keywords:** Biocatalyst; Carbonate solution; Chemical CO<sub>2</sub> absorption, Enzyme, HFMC; Modelling

## 1. Introduction

Climate challenges today are mainly caused by global warming, changes in natural ecosystems, and economic and technological problems. Global warming is primarily driven by the gradual rise in Earth's average temperature. This rise in temperature is mostly due to greenhouse gas (GHG) emissions, especially carbon dioxide (CO<sub>2</sub>). GHGs are mainly released by the fossil fuel, petrochemical, steel, transport, and cement industries. CO<sub>2</sub> is known to be one of the main drivers of climate change. Its level in the atmosphere has grown quickly in recent years, mostly because of the widespread use of fossil fuels (Sekartadji *et al.* 2023; Muthumari *et al.* 2024). Global climate change is largely influenced by complex atmospheric dynamics and the accumulation of greenhouse gases, particularly carbon dioxide (CO<sub>2</sub>). These disturbances directly affect ecosystems, human health, agriculture, and global climate stability (Nirmal, Subramanian and Surendran, 2025), a substantial growth of CO<sub>2</sub> emissions over the past 150 years has resulted in a significant increase of the atmospheric CO<sub>2</sub> concentration. The remarkable upward trend in Earth's average temperature could threaten human health, lives and industries associated with the temperature rise (Ze and Sx, 2014a). Climate change is leading to an increase in extreme weather events such as wildfires, heat waves and droughts, threatening ecosystems, food security and human health. In response to this crisis, reducing CO<sub>2</sub> emissions particularly through advanced technologies (Jasmine *et al.* 2025). Hollow fiber Membrane contactor (HFMC) has emerged as an innovative alternative, offering numerous advantages such as prevention of interphase dispersion, a high specific surface area, and a compact design (Ze and Sx, 2014; Mansourizadeh *et al.* 2022). Membrane gas absorption has recently attracted much attention as one of the promising

technologies for CO<sub>2</sub> capture because of its superior mass transfer efficiency high surface-to-volume ratio, flexible operation, modularity, compact design, and linear scalability (Okabe, Mano and Fujioka, 2008; Han and Ho, 2018). Alkanolamine solvents, such as MEA, are commonly used for CO<sub>2</sub> capture due to their rapid reaction rate with CO<sub>2</sub>. However, they are associated with high regeneration energy demands and evaporative losses (Zare, Keshavarz and Mowla, 2019). To overcome these drawbacks, other absorbents have been tried, one of which is carbonate aqueous solution. Carbonate solution is inexpensive, noncorrosive, and its regeneration for CO<sub>2</sub> capture consumes less energy compared to MEA. However, it also presents a smaller reaction rate with CO<sub>2</sub>, especially at low temperature and low partial pressure (Hu et al. 2016). A feasible way to improve the performance of carbonate solution (e.g., K<sub>2</sub>CO<sub>3</sub>, Na<sub>2</sub>CO<sub>3</sub>) is to add reaction promoters in it. Carbonic anhydrase is an extremely effective catalyst and promoter discovered in 1933 from red blood cells (Maćkowiaka et al. 2018), which catalyzes the reversible conversion of CO<sub>2</sub> to HCO<sub>3</sub><sup>-</sup>. Traditional CO<sub>2</sub> capture methods consume a lot of energy and degrade over time. Enzyme-enhanced absorption may solve these problems and provide a greener, faster, and cheaper method.

The aim of this research is to investigate and improve the efficiency of enzyme (bio-promoter) on CO<sub>2</sub> capture in carbonate solution using hollow fiber membrane contactor. This work evaluates To simulate the process using COMSOL, study of the effect of adding an enzyme on CO<sub>2</sub> absorption and key parametric study performance on HFMC, such as gas and liquid flow rate.

With a focus on evaluating the effect of an industrial enzyme, α-carbonic anhydrase from Bovine "Carbonic anhydrase" (bCA), to accelerate the process of capture using HFMC. bCA was selected for exceptional catalytic efficiency. The enzyme's kinetic data,  $k_e$  from the study by (Alper and Deckwer, 1980a). The study investigates CO<sub>2</sub> absorption using carbonate solutions, both with and without the addition of the enzyme, through process simulation supported in a hollow fiber membrane contactor. This innovative approach aims to enhance CO<sub>2</sub> capture efficiency and promote the sustainability of carbon capture processes

## 2. Membrane description and transport equation modeling for CO<sub>2</sub> capture

**Figure 1** illustrates a schematic of module and a single hollow fiber membrane, showing the directions of liquid and gas fluxes. It includes a view depicting the fiber's radius used in this study.

The key assumptions made to simplify mass transfer calculations in the numerical model development are as follows:

- Steady-state conditions are assumed,
- The system operates under isothermal conditions,
- Fully developed velocity profiles for gas and liquid phases are considered within,
- Co-current and counter-current are taken into account,

- Only CO<sub>2</sub> is transferred through the membrane into the tube side (no wetted for pores),
- Michaelis-Menten kinetics are applied to describe the enzymatic reaction rate of with CO<sub>2</sub> in the carbonate solution.

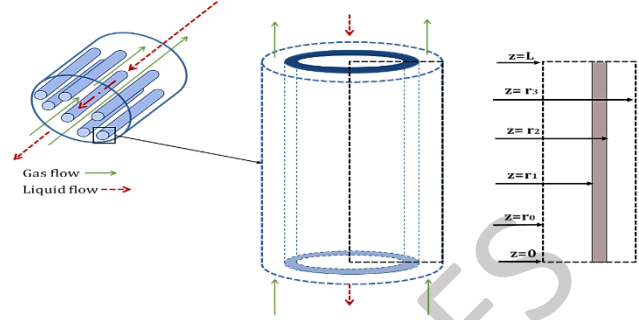


**Figure 1.** Depict a schematic diagram related to a CO<sub>2</sub> absorption process through HFMC.

### 2.1. Shell side equations

The steady-state mass transfer equation in the shell side in cylindrical coordinates is then derived as (Faiz and Al-Marzouqi, 2009)

$$D_{CO_2,shell} \left[ \frac{\partial^2 C_{CO_2,shell}}{\partial r^2} + \frac{1}{r} \frac{\partial C_{CO_2,shell}}{\partial r} + \frac{\partial^2 C_{CO_2,shell}}{\partial z^2} \right] = V_{z,shell} \frac{\partial C_{CO_2,shell}}{\partial z} \quad (1)$$

Boundary conditions for shell side equations in counter-current are given as

$$at \ z = 0, C_{CO_2-shell} = C_0 \quad (2)$$

$$at \ z = L, \frac{\partial C_{CO_2,shell}}{\partial z} = 0 \quad (3)$$

$$at \ r = r_3, \frac{\partial C_{CO_2,shell}}{\partial r} = 0 \text{ (insulated)} \quad (4)$$

$$at \ r = r_2, C_{CO_2-shell} = C_{CO_2-membrane} \quad (5)$$

Assuming Happel's free surface model (Happel, 1959), the velocity profile in the shell is given by

$$V_{z-shell} = 2V \left[ 1 - \left( \frac{r_2}{r_3} \right)^2 \right] \times \frac{\left( \frac{r}{r_3} \right)^2 - \left( \frac{r_2}{r_3} \right)^2 + 2 \ln \left( \frac{r_2}{r} \right)}{3 + \left( \frac{r}{r_3} \right)^4 - 4 \left( \frac{r_2}{r_3} \right)^2 + 4 \ln \left( \frac{r_2}{r_3} \right)} \quad (6)$$

### 2.2. Membrane side equations

The steady state continuity equation for the transport of CO<sub>2</sub> inside membrane with cylindric coordinates, taken only radial diffusion (no wetted pores), can be written as (Shirazian et al. 2020):

$$D_{CO_2,membrane} \left[ \frac{\partial^2 C_{CO_2,membrane}}{\partial r^2} + \frac{1}{r} \frac{\partial C_{CO_2,membrane}}{\partial r} + \frac{\partial^2 C_{CO_2,membrane}}{\partial z^2} \right] = 0 \quad (7)$$

$$D_{CO_2,membrane} = \varepsilon \frac{D_{CO_2,shell}}{\tau} \quad (8)$$

$$\tau = \frac{(2-\varepsilon)^2}{\varepsilon} \quad (9)$$

Boundary conditions are given as

$$\text{at } r = r_2, C_{\text{CO}_2\text{-shell}} = C_{\text{CO}_2\text{-membrane}}, \quad (10)$$

$$\text{at } r = r_1, C_{\text{CO}_2\text{-membrane}} = \frac{C_{\text{CO}_2\text{-tube}}}{m}. \quad (11)$$

### 2.3. Tube side equations

On the tube side, there is reaction for CO<sub>2</sub> in carbonate solution with enzyme, the transmission continuity equation is as follows (Shirazian *et al.* 2020):

$$D_{\text{CO}_2, \text{tube}} \left[ \frac{\partial^2 C_{\text{CO}_2, \text{tube}}}{\partial r^2} + \frac{1}{r} \frac{\partial C_{\text{CO}_2, \text{tube}}}{\partial r} + \frac{\partial^2 C_{\text{CO}_2, \text{tube}}}{\partial z^2} \right] = V_{z, \text{tube}} \frac{\partial C_{\text{CO}_2, \text{tube}}}{\partial z} - R_{\text{CO}_2} \quad (12)$$

Boundary conditions for tube side equations in counter-current flow are given as

$$\text{at } z = 0, \frac{\partial C_{\text{CO}_2, \text{Shell}}}{\partial z} = 0, \quad (13)$$

$$\text{at } z = L, C_{\text{solvent}} = C_0, \quad (14)$$

$$\text{at } r = r_1, C_{\text{CO}_2\text{-tube}} = m \times C_{\text{CO}_2\text{-membrane}}, \quad (15)$$

Boundary conditions for tube side equations in co-current flow are given as

$$\text{at } z = 0, C_{\text{solvent}} = C_0, \quad (16)$$

$$\text{at } z = L, \frac{\partial C_{\text{CO}_2\text{-tube}}}{\partial z} = 0, \quad (17)$$

$$\text{at } r = r_1, C_{\text{CO}_2\text{-tube}} = m \times C_{\text{CO}_2\text{-membrane}}. \quad (18)$$

It is hypothesized that the velocity distribution within the tube will be in accordance with Newtonian laminar flow (Bird, 1960)

$$V_{z, \text{tube}} = 2\bar{V}_T \left[ 1 - \left( \frac{r}{r_1} \right)^2 \right] \quad (19)$$

$$\bar{V}_T = \frac{Q_1}{n\pi(r_1)^2} \quad (20)$$

The  $r_3$  on the shell side, part of the membrane contactor can be estimated by the development of fluid around the fiber, the area of the free void can be predicted by Happel's free surface model (Srisurichan, Jiratananon and Fane, 2006).

$$r_3 = \left( \frac{1}{1-\phi} \right)^{1/2} r_2 \quad (21)$$

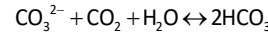
Where  $\phi$  is the volume fraction of the vacuum in the module, It can be calculated as follows (Happel, 1959).

$$1-\phi = \frac{nr_2^2}{R^2} \quad (22)$$

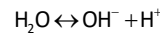
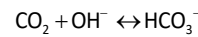
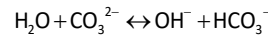
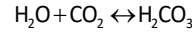
where  $n$  is the number of fibers, and  $R$  is the module's inner radius.

### 3. Kinetics of CO<sub>2</sub> with carbonate solution

The global reactions between CO<sub>2</sub> and carbonate solution are presented as follows (Pohorecki and Moniuk, 1988):



The above reaction is evidently made up of a sequence of elementary steps. The carbonate ion first reacts with water to generate hydroxyl ions, which then react with CO<sub>2</sub> as follows (Astarita, Savage and Longo, 1981).



Aqueous carbon dioxide may react with water to form bicarbonate as shown in *Reaction 2*. The contribution of this reaction to the overall absorption of CO<sub>2</sub> is usually assumed to be negligible in basic solutions. Additionally, since *Reaction 3* is an instantaneous reaction, *Reaction 4* is the limiting reaction. So, the rate equation of CO<sub>2</sub> with hydroxyl ion (*Reaction 4*) expresses as (Thee, 2013).

$$R_{(\text{CO}_2)} = k_{\text{OH}} [\text{OH}^-] ([\text{CO}_2] - [\text{CO}_{2e}]) \quad (23)$$

We can consider  $[\text{CO}_{2e}] = [\text{CO}_{2b}]$ , with  $[\text{CO}_{2e}]$  is equilibrium concentration of CO<sub>2</sub>,  $[\text{CO}_{2b}]$  is concentration of CO<sub>2</sub> in the bulk, since that the solution is alkaline (pH > 9), CO<sub>2</sub> concentration in the bulk can be negligible. So, we can write the reaction rate of CO<sub>2</sub> as follows (Russo *et al.* 2013):

$$R_{(\text{CO}_2)} = (k_w + k_{\text{OH}} - [\text{OH}^-]) [\text{CO}_{2, \text{tube}}] \quad (24)$$

Where  $R_{(\text{CO}_2)}$  is the rate of reaction (mol m<sup>-3</sup> s<sup>-1</sup>),  $k_{\text{OH}}$  is the second order rate constant, and  $[\text{CO}_{2, \text{tube}}]$  and  $[\text{OH}^-]$  are the concentrations of free CO<sub>2</sub> and base in the liquid phase. The second order rate constant of reaction of CO<sub>2</sub> with OH<sup>-</sup> and constant of water can be found from Equation 24 and Equation 25 (Danckwerts, 1966; Afza, Hashemifard and Abbasi, 2018).

$$\log k_{\text{OH}} = 13.635 - \frac{2895}{T} \quad (25)$$

$$\log k_w = 329.85 - 110.541 \log(T) - \frac{17265.4}{T} \quad (26)$$

Where C<sub>1</sub>, C<sub>2</sub>, and C<sub>3</sub> are constant and equal to 2.61 × 10<sup>-4</sup> (m<sup>3</sup> mol<sup>-1</sup>), 1.40 × 10<sup>-4</sup> (m<sup>3</sup> mol<sup>-1</sup>), and 1.29 × 10<sup>-4</sup> (m<sup>3</sup> mol<sup>-1</sup>), respectively like it mentioned in Table 1. Diffusion coefficient  $D_{\text{CO}_2, 0}$  of CO<sub>2</sub> in water at 298 K is 1.88 × 10<sup>-9</sup> (m<sup>2</sup> s<sup>-1</sup>) (Versteeg, Blauwhoff and van Swaaij, 1987).

**Table 1.** Physical parameters used in this work.

Parameters	Expression	References
$D_{CO_2, tube}$	$1 - \left( C1 \left[ CO_3^{2-} \right] + C2 \left[ HCO_3^- \right] + C3 \left[ OH^- \right] \right) \times D_{CO_2, 0}$	(Versteeg, Blauwhoff and van Swaaij, 1987)
$m_{0, CO_2}$	$3.59 \times 10^{-7} RT e^{\left( \frac{2044}{T} \right)}$	(Dindore, Brilman and Versteeg, 2005)
$\log(m_0 / m')$	$\Sigma(h_{i+} + h_G) C_i$	(Weisenberger and Schumpe, 1996)
$h_G$	$h_{G,0} + 0.338 \times 10^{-3} (T - 298.15)$	(Weisenberger and Schumpe, 1996)

**Table 2.** Constants  $h_{i+}$  used in this work (Weisenberger and Schumpe, 1996).

Constant	Value
$h_{CO_2}$	-0.0172
$h_{HCO_3^-}$	0.0967
$CO_3^{2-}$	0.1423

**Table 3.** Characteristics of HFMC module and fluid specification used in this work (Poling, Prausnitz and O'connell, 2001; Cao *et al.* 2021).

Parameters	value	Unit
Fiber length (L)	0.210	m
Number of fibers (n)	11	-
Membrane inner diameter ( $r_1$ )	$2.1 \times 10^{-4}$	m
Membrane outer diameter ( $r_2$ )	$5.5 \times 10^{-4}$	m
Module inner diameter ( $r_3$ )	0.004	m
Membrane thickness ( $\delta$ )	$3.4 \times 10^{-4}$	m
$D_{CO_2, Shell}$	$1.39 \times 10^{-5}$	m <sup>2</sup> /s
$D_{CO_2, membrane}$	$D_{CO_2, Shell} * (\epsilon / \tau)$	m <sup>2</sup> /s
$D_{CO_2, tube}$ (caculated)	$1.75 \times 10^{-9}$	m <sup>2</sup> /s
Henry's law physical constant $m'$ (calculated)	0.66	-

#### 4. Kinetics of CO<sub>2</sub> with Carbonic Anhydrase (CA)

The catalyzed mechanism of Carbonic anhydrase (CA) for CO<sub>2</sub> hydration was introduced by (Lindskog and Silverman, 2000a, 2000b). CA is an efficient hydration catalyst and its reaction with CO<sub>2</sub> had been studied, the main reactions of CA with CO<sub>2</sub> are expressed in equation (20), equation (21) (Lindskog and Silverman, 2000a).



The enzymatic reaction which takes the form of a first order Michaelis-Menten equation, expressed as follows

$$R_{CA} = k_e [E] [CO_{2, tube}] \quad (27)$$

With  $R_{CA}$  (mol m<sup>-3</sup> s<sup>-1</sup>) is the reaction rate of enzyme bCA with CO<sub>2</sub>,  $k_e$  (m<sup>3</sup> mol<sup>-1</sup> s<sup>-1</sup>) or (m<sup>3</sup> kg<sup>-1</sup> s<sup>-1</sup>) is the first order Michaelis-Menten kinetic,  $[E]$  is enzyme concentration (kg m<sup>-3</sup>) or (mol m<sup>-3</sup>).

For bCA enzyme, the  $k_e$  is 1.15 (L mg<sup>-1</sup> s<sup>-1</sup>) (Alper and Deckwer, 1980a).

In this work the reaction rate of CO<sub>2</sub> with enzyme and carbonate solution can expressed as:

$$R_{CO_2} = (k_e [E] + k_w + k_{OH} - [OH^-]) [CO_{2, tube}] \quad (28)$$

Materiel chosen for the membrane is PVDF from (Cao *et al.* 2021), the dimension of fiber and module of membrane are listed in Table 3, also for porosity and tortuosity are 0.4585 and 5.18 respectively.

#### 5. Numerical solution

A set of governing partial differential equations of CO<sub>2</sub> mass transfer from gas phase (Shell side) passing through hollow fibers contactor using carbonate solution with bCA in liquid phase (Tube side), were solved based on finite elements method (FEM) by COMSOL Multiphysics software (Version 5.0), which can divide different domains in the hollow fiber membrane contactor into small dimension units to obtain the simulated results of important parameters such as CO<sub>2</sub> concentration profiles at each point of the domains. Overview of CO<sub>2</sub> gas capture using HFMC mentioned in Table 4. The Specifications of membrane and the related physical and chemical parameters are listed in Table 1, Table 2 and Table 3, respectively. An internal numerical solver of COMSOL, PARDISO, is employed to achieve self-adaptive meshing and error control were employed to minimize the calculations errors (Pishnamazi *et al.* 2020).

**Table 4.** Overview of recent advancements in CO<sub>2</sub> gas capture using hollow fiber membrane.

Membrane	Absorbent Solution	Gas Mixture	Absorption Flux (mol/m <sup>2</sup> .s)	References
Polyvinylidene fluoride (PVDF)	Nanofluid of MDEA + CNT	CO <sub>2</sub> /N <sub>2</sub> (20/80)	1.14×10 <sup>-3</sup>	(Cao <i>et al.</i> 2021)
PP (3M Liqui-Cel™)	Potassium glycinate amino acid salt	CO <sub>2</sub> /N <sub>2</sub> (10/90)	2.27×10 <sup>-4</sup>	(Nieminen <i>et al.</i> 2020)
Superhydrophobic PEEK	Activated K <sub>2</sub> CO <sub>3</sub>	CO <sub>2</sub> /N <sub>2</sub> (13/87)	2.5×10 <sup>-3</sup>	(Li <i>et al.</i> 2013)
Polyvinylidene fluoride (PVDF)	Carbonate solution + bCA	(20/80)	2.44×10 <sup>-4</sup>	This work

## 6. Results and discussions

A simulation using a CO<sub>2</sub> capture using carbonate solvent with carbonic anhydrase in a counter-current and co-current using hollow fiber membrane contactor is given. The main parameters study is; Effects of enzyme concentration, gas and liquid flow rate on CO<sub>2</sub> removal efficiency have been investigated in this study.

$$\text{CO}_2\text{removal\%} = 100 \times \frac{(Q \times C)_{\text{inlet}} - (Q \times C)_{\text{outlet}}}{(Q \times C)_{\text{inlet}}} \quad (29)$$

$$= 100 \times \left( 1 - \frac{C_{\text{outlet}}}{C_{\text{inlet}}} \right)$$

In this equation,  $Q_g$  and  $C$  represent the volumetric flow rate and the concentration, respectively. Assuming that the maximum concentration of CO<sub>2</sub> in the gas mixture at the inlet is 20%, it can be concluded that the variation in volumetric flow rate is negligible. This allows for the approximation of CO<sub>2</sub> removal with this equation.

### 6.1. Velocity profile

Figure 3 depicts the gas and liquid velocity profile on the shell side and tube side expressed as Equation 2 and Equation 3 Respectively, Figure 3 demonstrates that the fully developed velocity profile is confirmed by the previously stated assumption.

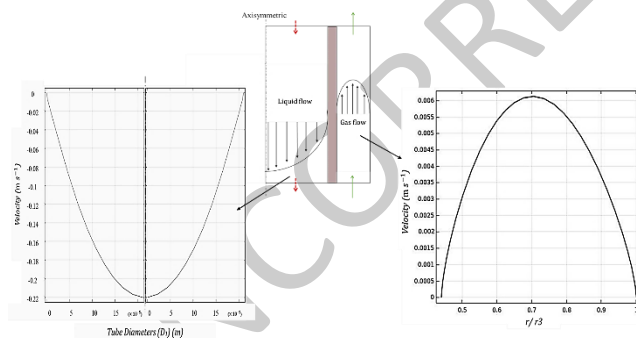


**Figure 2.** Gas and liquid velocity profile,  $Q_l = 10 \text{ ml min}^{-1}$ ,  $Q_g = 10 \text{ ml min}^{-1}$

### 6.2. Gas flow rate effect on CO<sub>2</sub> removal

Figure 3 illustrates the relationship between gas flow rate of CO<sub>2</sub> and removal efficiency for 0.5M Carbonate solution (Na<sub>2</sub>CO<sub>3</sub>-NaHCO<sub>3</sub>), pure and with the bCA (5 mg L<sup>-1</sup>). Figure 3.a shows that increasing the gas flow rate of CO<sub>2</sub> from 10 mL min<sup>-1</sup> to 40 mL min<sup>-1</sup> reduces CO<sub>2</sub> removal from 23.47 % to 6.68% in pure solution, whereas with 5 mg L<sup>-1</sup> of bCA increasing the gas flow rate of CO<sub>2</sub> from 10 mL min<sup>-1</sup> to 40 mL min<sup>-1</sup> reduces CO<sub>2</sub> removal from 57.17 % to 19.79 %. An increase in gas flow rate of CO<sub>2</sub> reduces the contact time between CO<sub>2</sub> and the absorbing liquid, which decreases the capture efficiency. CO<sub>2</sub> absorption is often limited by mass

transfer between the gas and liquid phases. However, the bCA enzyme helps to overcome this limitation by maintaining a high CO<sub>2</sub> concentration gradient and accelerating the chemical reaction, thereby increasing absorption. Figure 3.b shows that increasing the gas flow rate from 10 to 40 mL/min reduces the removal efficiency in both co-current and counter-current flow. However, counter current flow improves efficiency by an average of 3% by maintaining a high concentration gradient, optimising mass transfer and increasing gas-liquid contact time, resulting in better CO<sub>2</sub> capture.

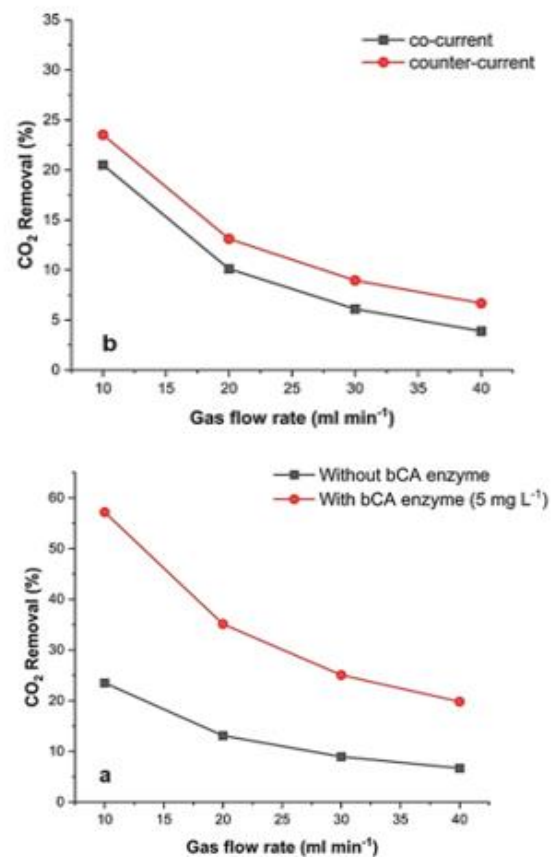


**Figure 3.** CO<sub>2</sub> removal as function of gas flow rate,  $C_{\text{CO}_2} = 5.24 \text{ mol m}^{-3}$ , bCA enzyme concentration = 5 mg L<sup>-1</sup>,  $Q_l = 10 \text{ ml min}^{-1}$ , 0.5M (Na<sub>2</sub>CO<sub>3</sub>-NaHCO<sub>3</sub>), T=298 K, pH= 9.6

### 6.3. Liquid flow rate effect on CO<sub>2</sub> removal

Figure 4 shows the impact of liquid flow rate on CO<sub>2</sub> removal efficiency with and without enzyme in 0.5 M Carbonate solution (Na<sub>2</sub>CO<sub>3</sub>-NaHCO<sub>3</sub>). Figure 4.a shows that as the liquid flow rate increases from 10 mL min<sup>-1</sup> to 40 mL min<sup>-1</sup> CO<sub>2</sub> removal increase from 23.47 % to 56.33 % without addition of bCA. With 5 mg/L of bCA it finds that CO<sub>2</sub> removal increase from 57.17 % to 69.07 %. This



enhancement (~24 % to ~14 %), from 10 mL min<sup>-1</sup> to 40 mL min<sup>-1</sup> (the main causes of the decrease in effectiveness are the solvent's saturation with CO<sub>2</sub> and the shorter contact time) due to bCA which lowers the mass transfer resistance by speeding up the process. The enhancement is more noticeable at high flow rates, indicating that the enzyme enhances absorption even more at high liquid renewal rates. Figure 4.b increasing in liquid flow rate from 10 mL min<sup>-1</sup> to 40 mL min<sup>-1</sup> both in counter-current and co-current, removal efficiency increase, here the counter-current flow enhances removal efficiency about ~3 %.

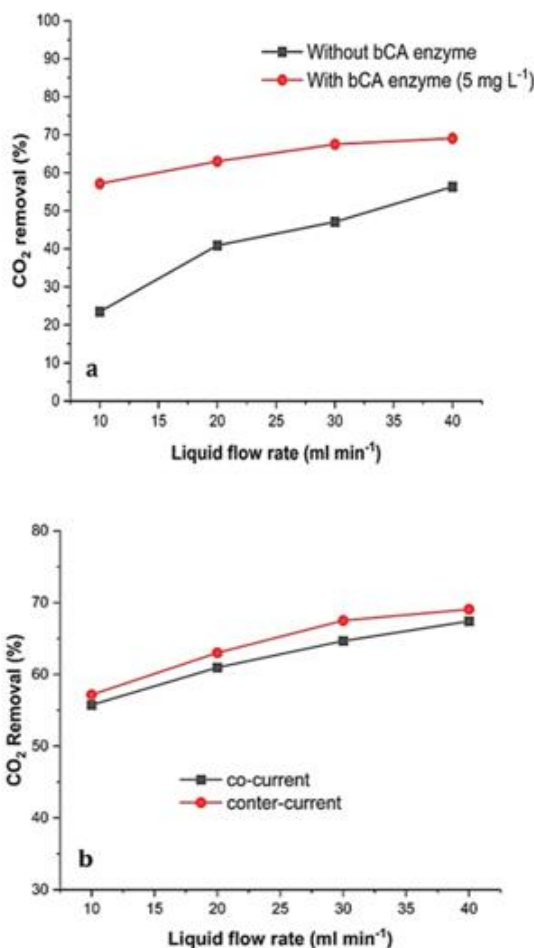


**Figure 4.** CO<sub>2</sub> removal as function of gas flow rate,  $C_{\text{CO}_2} = 5.24$  mol m<sup>-3</sup>, bCA enzyme = 5 mg L<sup>-1</sup>,  $Q_g = 10$  ml min<sup>-1</sup>, 0.5M (Na<sub>2</sub>CO<sub>3</sub>-NaHCO<sub>3</sub>), T = 298 K, pH=9.6

#### 6.4. Effect of enzyme bCA

Figure 5 presents the effect of concentration of bCA on CO<sub>2</sub> removal efficiency. An increase in CO<sub>2</sub> removal is observed from 23.17% to 91.51%, when bCA concentration increases from 0 mg L<sup>-1</sup>, to 50 mg L<sup>-1</sup> respectively. Figure 5 shows that with 5 mg L<sup>-1</sup> of bCA the efficiency of CO<sub>2</sub> removal intensifies by average 24%. The use of bCA enzyme has a notable impact by accelerating the CO<sub>2</sub> hydration reaction, which significantly increasing the effectiveness of the capture process. Beyond this concentration (40 mg L<sup>-1</sup>), the efficiency stabilizes, showing no significant further improvement. bCA enzyme improves mass transfer by maintaining a high concentration gradient, which implies a reduction in transfer resistance in the carbonate solution. From about 40 mg L<sup>-1</sup>, the improvement CO<sub>2</sub> removal

efficiency becomes very weak, indicating an enzyme saturation effect. Adding more enzyme beyond 40 mg L<sup>-1</sup> hardly improves performance anymore.

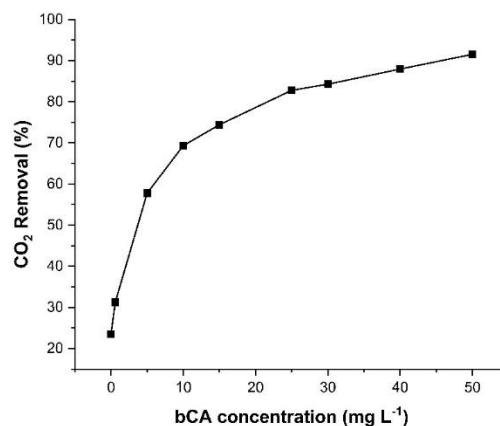


**Figure 5.** CO<sub>2</sub> removal as function of bCA enzyme concentration,  $C_{\text{CO}_2} = 5.24$  mol m<sup>-3</sup>, T= 298 K, pH= 9.6,  $Q_l = 10$  ml min<sup>-1</sup>,  $Q_g = 10$  ml min<sup>-1</sup>, n=11, Counter-current flow

## 7. Conclusions

In conclusion, this thesis explores the modelling and simulation of CO<sub>2</sub> capture using a hollow fiber membrane with carbonate solutions enhanced by enzymes as bio-promoters. The developed methodology has been successfully implemented, providing valuable insights into the theoretical impact of enzymatic enhancement on CO<sub>2</sub> absorption efficiency using, for COMSOL software. Key parameters studied such as the gas flow rate, liquid flow rate both in counter-current and co-current, enzyme concentration. It founds that increasing the CO<sub>2</sub> gas flow rate from 10 ml min<sup>-1</sup> to 40 ml min<sup>-1</sup>, reduces removal efficiency due to decreased contact time and mass transfer limitations, increasing the liquid flow rate from 10 ml min<sup>-1</sup> to 40 ml min<sup>-1</sup> CO<sub>2</sub> removal efficiency increases. However, the presence of the bCA enzyme and the counter-current flow configuration enhance CO<sub>2</sub> absorption both in term of gas and liquid flow rate by maintaining a high concentration gradient Although the bCA enzyme improves CO<sub>2</sub> removal efficiency, its impact becomes less significant at higher flow rates, as physical mass transfer limitations start to dominate over reaction kinetics. Additionally. The bCA enzyme significantly enhances CO<sub>2</sub> removal in carbonate solutions, reaching nearly almost total removal efficiency at 40 mg L<sup>-1</sup> enzyme concentration.

## Abbreviations

C	Concentration (mol m <sup>-3</sup> )
bCA	Bovine Carbonic Anhydrase
C <sub>CO<sub>2</sub></sub>	Concentration (mol m <sup>-3</sup> )
C <sub>0</sub>	CO <sub>2</sub> concentration at inlet (mol m <sup>-3</sup> )
C <sub>CO<sub>2</sub>,shell</sub>	CO <sub>2</sub> concentration in the shell side (mol m <sup>-3</sup> )
C <sub>CO<sub>2</sub>,membrane</sub>	CO <sub>2</sub> concentration in the membrane side (mol m <sup>-3</sup> )
C <sub>CO<sub>2</sub>,tube</sub>	CO <sub>2</sub> concentration in the tube side (mol m <sup>-3</sup> )

$D_{CO_2, \text{shell}}$	Diffusion constant of CO <sub>2</sub> in the shell side (m <sup>2</sup> s <sup>-1</sup> )
$C_{CO_2, \text{membrane}}$	Diffusion constant of CO <sub>2</sub> in the membrane side (m <sup>2</sup> s <sup>-1</sup> )
$D_{CO_2, \text{tube}}$	Diffusion constant of CO <sub>2</sub> in tube side (m <sup>2</sup> s <sup>-1</sup> )
HFMC	Hollow fiber membrane contactor
$k_{OH^-}$	Specific reaction rate constant of amine (m <sup>3</sup> kmol <sup>-1</sup> s <sup>-1</sup> )
$k_{cat}$	Turnover Number (s <sup>-1</sup> )
$k_m$	Michaelis Constant (mol m <sup>-3</sup> )
$L$	Length of the fiber (m)
$m'$	Physical solubility
$n$	Number of fibers
$Q_l$	Liquid flow rate (m <sup>3</sup> s <sup>-1</sup> )
$Q_g$	Gas flow rate of CO <sub>2</sub> (m <sup>3</sup> s <sup>-1</sup> )
$R$	Module radius (m)
$r_1$	Outer membrane radius (m)
$r_2$	Inner membrane radius (m)
$r_3$	Shell radius (m)
$\bar{V}$	Average velocity (m s <sup>-1</sup> )
$V_{z, \text{shell}}$	Velocity in the shell side (m s <sup>-1</sup> )
$V_{z, \text{tube}}$	Velocity in the tube side (m s <sup>-1</sup> )
$\phi$	Module volume fraction
$\delta$	Thickness
$\varepsilon$	Porosity
$\tau$	Tortuosity factor

## References

- Afza, K.N., Hashemifard, S.A. and Abbasi, M. (2018) 'Modelling of CO<sub>2</sub> absorption via hollow fiber membrane contactors: Comparison of pore gas diffusivity models', *Chemical Engineering Science*, **190**, 110–121.
- Alper, E. and Deckwer, W.-D. (1980a) 'Kinetics of absorption of CO<sub>2</sub> into buffer solutions containing carbonic anhydrase', *Chemical Engineering Science*, **35**(3), 549–557.
- Alper, E. and Deckwer, W.-D. (1980b) 'Kinetics of absorption of CO<sub>2</sub> into buffer solutions containing carbonic anhydrase', *Chemical Engineering Science*, **35**(3), 549–557.
- Astarita, G., Savage, D.W. and Longo, J.M. (1981) 'Promotion of CO<sub>2</sub> mass transfer in carbonate solutions', *Chemical Engineering Science*, **36**(3), 581–588.
- Bird R.B. (1960) 'We stewart, and en lightfoot', *Transport phenomena*, **11**, 5.
- Cao, Y. et al. (2021) 'Intensification of CO<sub>2</sub> absorption using MDEA-based nanofluid in a hollow fibre membrane contactor', *Scientific Reports*, **11**(1), 2649.
- Danckwerts, P.V. (1966) 'The absorption of carbon dioxide into solutions of alkalis and amines', *Chemical Engineering*. Available at: <https://cir.nii.ac.jp/crid/1570854174139087360> (Accessed: 15 March 2025).
- Dindore, V.Y., Brilman, D.W.F. and Versteeg, G.F. (2005) 'Modelling of cross-flow membrane contactors: Mass transfer with chemical reactions', *Journal of Membrane Science*, **255**(1–2), 275–289.
- Faiz, R. and Al-Marzouqi, M. (2009) 'Mathematical modeling for the simultaneous absorption of CO<sub>2</sub> and H<sub>2</sub>S using MEA in hollow fiber membrane contactors', *Journal of Membrane Science*, **342**(1–2), 269–278.
- Han, Y. and Ho, W.W. (2018) 'Recent advances in polymeric membranes for CO<sub>2</sub> capture', *Chinese Journal of Chemical Engineering*, **26**(11), 2238–2254.
- Happel, J. (1959) 'Viscous flow relative to arrays of cylinders', *AIChE Journal*, **5**(2), 174–177. Available at: <https://doi.org/10.1002/aic.690050211>.
- Hu, G. et al. (2016) 'Carbon dioxide absorption into promoted potassium carbonate solutions: A review', *International Journal of Greenhouse Gas Control*, **53**, 28–40.
- Jasmine, J. et al. (2025) 'Advanced Weather Prediction based on Hybrid Deep Gated Tobler's Hiking Neural Network and robust Feature Selection for tackling Environmental Challenges', *Global NEST Journal*. Available at: <https://doi.org/10.30955/gnj.06757>.
- Li, S. et al. (2013) 'Post-combustion CO<sub>2</sub> capture using super-hydrophobic, polyether ether ketone, hollow fiber membrane contactors', *Journal of Membrane Science*, **430**, 79–86.
- Lindskog, S. and Silverman, D.N. (2000a) 'The catalytic mechanism of mammalian carbonic anhydrases', in W.R. Chegwidden, N.D. Carter, and Y.H. Edwards (eds) *The Carbonic Anhydrases*. Basel: Birkhäuser Basel, 175–195. Available at: [https://doi.org/10.1007/978-3-0348-8446-4\\_10](https://doi.org/10.1007/978-3-0348-8446-4_10).
- Lindskog, S. and Silverman, D.N. (2000b) 'The catalytic mechanism of mammalian carbonic anhydrases', in W.R. Chegwidden, N.D. Carter, and Y.H. Edwards (eds) *The Carbonic Anhydrases*. Basel: Birkhäuser Basel, 175–195. Available at: [https://doi.org/10.1007/978-3-0348-8446-4\\_10](https://doi.org/10.1007/978-3-0348-8446-4_10).
- Maćkowiaka, J.F. et al. (2018) 'Absorption of carbon dioxide using enzyme activated amine solution in columns with random packings', *Chemical Engineering*, 69. Available at: <https://folk.ntnu.no/skoge/prost/proceedings/Distillation&Absorption-2018/papers/52mackowiak.pdf> (Accessed: 15 March 2025).
- Mansourizadeh, A. et al. (2022) 'A review on recent progress in environmental applications of membrane contactor technology', *Journal of Environmental Chemical Engineering*, **10**(3), 107631.
- Muthumari, P. et al. (2024) 'A comprehensive review on CO<sub>2</sub> capture process using amine-ionic liquids mixtures', *Global Nest Journal*, **26**(9).
- Nieminen, H. et al. (2020) 'Insights into a membrane contactor based demonstration unit for CO<sub>2</sub> capture', *Separation and Purification Technology*, **231**, 115951.
- Nirmal, K.M., Subramanian, P. and Surendran, R. (2025) 'Multivariate time series weather forecasting model using integrated secondary decomposition and Self-Attentive spatio-temporal learning network', *Global NEST Journal*, **27**(4). Available at: <https://doi.org/10.30955/gnj.06195>.
- Okabe, K., Mano, H. and Fujioka, Y. (2008) 'Separation and recovery of carbon dioxide by a membrane flash process', *International Journal of Greenhouse Gas Control*, **2**(4), 485–491.
- Pishnamazi, M. et al. (2020) 'Molecular investigation into the effect of carbon nanotubes interaction with CO<sub>2</sub> in molecular separation using microporous polymeric membranes', *Scientific Reports*, **10**(1), 13285.
- Pohorecki, R. and Moniuk, W. (1988) 'Kinetics of reaction between carbon dioxide and hydroxyl ions in aqueous electrolyte solutions', *Chemical Engineering Science*, **43**(7), 1677–1684.
- Poling, B.E., Prausnitz, J.M. and O'Connell, J.P. (2001) *The properties of gases and liquids*. McGraw-hill New York. Available at: [https://www.academia.edu/download/62015682/Prausnitz\\_-\\_Properties\\_of\\_Gases\\_and\\_Liquids20200206-55970-35et18.pdf](https://www.academia.edu/download/62015682/Prausnitz_-_Properties_of_Gases_and_Liquids20200206-55970-35et18.pdf) (Accessed: 15 March 2025).

- Russo, M.E. et al. (2013) 'Post-combustion carbon capture mediated by carbonic anhydrase', *Separation and Purification Technology*, **107**, 331–339.
- Sekartadji, R. et al. (2023) 'CO<sub>2</sub> emission of aircraft at different flight-level (route: Jakarta-surabaya)', *Chemical Engineering Transactions*, **98**, 39–44.
- Shirazian, S. et al. (2020) 'Theoretical investigations on the effect of absorbent type on carbon dioxide capture in hollow-fiber membrane contactors', *PLoS One*, **15**(7), e0236367.
- Srisurichan, S., Jiratananon, R. and Fane, A.G. (2006) 'Mass transfer mechanisms and transport resistances in direct contact membrane distillation process', *Journal of Membrane Science*, **277**(1–2), 186–194.
- Thee, H. (2013) Reactive absorption of carbon dioxide into promoted potassium carbonate solvents. PhD Thesis. *University of Melbourne, Department of Chemical and Biomolecular Engineering*. Available at: [https://minerva-access.unimelb.edu.au/bitstream/handle/11343/38619/307774\\_Hendy%20Thee\\_PhD%20Thesis\\_20140120s.pdf](https://minerva-access.unimelb.edu.au/bitstream/handle/11343/38619/307774_Hendy%20Thee_PhD%20Thesis_20140120s.pdf) (Accessed: 15 March 2025).
- Versteeg, G.F., Blauwhoff, P.M.M. and van Swaaij, W.P.M. (1987) 'The effect of diffusivity on gas-liquid mass transfer in stirred vessels. Experiments at atmospheric and elevated pressures', *Chemical Engineering Science*, **42**(5), 1103–1119.
- Weisenberger, S. and Schumpe, dan A. (1996) 'Estimation of gas solubilities in salt solutions at temperatures from 273 K to 363 K', *AIChE Journal*, **42**(1), 298–300.
- Zare, P., Keshavarz, P. and Mowla, D. (2019) 'Membrane Absorption Coupling Process for CO<sub>2</sub> Capture: Application of Water-Based ZnO, TiO<sub>2</sub>, and Multi-Walled Carbon Nanotube Nanofluids', *Energy & Fuels*, **33**(2), 1392–1403. Available at: <https://doi.org/10.1021/acs.energyfuels.8b03972>.
- Ze, Z. and Sx, J. (2014a) 'Hollow fiber membrane contactor absorption of CO<sub>2</sub> from the flue gas: review and perspective', *Global NEST Journal*, **16**, 355–374.
- Ze, Z. and Sx, J. (2014b) 'Hollow fiber membrane contactor absorption of CO<sub>2</sub> from the flue gas: review and perspective', *Global NEST Journal*, **16**, 355–374.